# DETAILED FIELD MEASUREMENTS OF FLOW CHARACTERISTICS ON THE RED RIVER

M. Goharrokhi[1] and S.P. Clark[1]

1. Department of Civil Engineering, University of Manitoba, Winnipeg, Manitoba, Canada

**ABSTRACT**: Sufficient resolution of measured flow data under different hydraulic conditions is of prime importance to develop an understanding of river processes and to enable accurate numerical modeling. The main objectives of this study were to obtain and assess a wide range of hydrometric and hydrodynamic data of the Red River in Winnipeg under varying flow conditions in order to develop calibrated hydrodynamic and sediment transport models. The numerical modelling results were combined with soil erodibility test results to perform bank erosion assessment and will facilitate the design of future erosion mitigation strategies in Winnipeg. Basic geometric parameters, water surface profile, dimensionless numbers (Froude, Reynolds), the stage-discharge rating curve, boundary friction coefficient, roughness height, and local and reach scale hydraulic shear stress were determined using the field data. An acoustic Doppler current profiler (ADCP) was used to collect spatial and temporal data along approximately 10 km of the Red River between the South Perimeter Bridge (SPB) and Fort Gary Bridge (FGB) over a 2 year period. High resolution water surface elevations at the reach extremes were also collected. These comprehensive results provide a better understanding and suitable knowledge for modelling of the complicated riverbank erosion phenomenon occurring on the Red. Collected data were also used to develop relationships between various hydraulic parameters and water surface elevations that can be used for practical applications.

## 1. INTRODUCTION

Extreme climatic events such as flooding have increased in frequency and magnitude in part due to recent changes in climate (IPCC, 2007). High flows are expected to increase river erodibility which will affect sediment production (Nam et al., 2010). The significant contribution of bank erosion to the total sediment load has been documented in previous studies (Trimble, 1997; Simon et al., 2000). The influence of bank erosion on water quality, contaminant transport, property loss, and aquatic as well as riparian ecosystems is the primary motivation for understanding bank erosion processes (Lawler et al., 1997; ASCE, 1998). These processes are generally controlled by river materials and flow properties. Cohesive riverbank materials exhibit complex behaviour due to the inter-particle forces that resist external forces applied by the flow. This behaviour is further complicated in cold regions (Formanek et al., 1984; Ferrick and Gatto, 2005). This study has been undertaken as part of a larger research program on cohesive riverbank erosion in Manitoba to provide further information on the Red River erosion processes. Accurate flow data (e.g. discharge, velocity, water depth) is a pre-requisite for understanding and modelling complicated river-related processes. A two dimensional hydrodynamic and sediment transport model, MIKE21 Flow model FM and MT, was calibrated based on the collected field data to evaluate the effect of different flow conditions on hydraulic shear stress. These shear stress results were combined with erosive properties of cohesive bank material of the Red River to perform flow induced erosion modelling. ADCP is capable of collecting the flow data, and by processing this data, desired hydraulic parameters can be investigated. Such parameters may include: depth-averaged velocity, velocity profile, shear velocity, shear stress, roughness height, and the roughness coefficient. The ADCP measures once per second and divides each water column sample into different cells. The ADCP can measure the instantaneous flow velocities in each cell by transmitting and receiving an acoustic signal at a set frequency into the water. It is assumed that suspended particles in a river which reflect the sound have the same velocity as the stream flow.

## 2. METHODOLOGY

Flow data collection was performed at 20 different cross sections along approximately 10 km of the Red River, between the SPB and FGB (Figure 1). Flow field measurements in the study reach were carried out more than 70 times from a boat or the SPB between 2012 and 2014. The main point of the extensive flow data collection was to observe the effect of the variation of water level on the spatial and temporal variability of flow properties. Throughout the study, velocity, depth, and discharge measurements were performed using a Sontek RiverSurveyor M9 with the Global Positioning System and Real-Time Kinematic (GPS-RTK) option. The GPS-RTK option provides precise positioning ($\pm 3$ cm) and timing information for data collection using satellite navigation techniques (Sontek, 2011). In conjunction with ADCP measurement, high resolution water surface elevations data at the reach extremes were analyzed. The SPB and FGB gauges measured the water level simultaneously every 15 and 10 minutes, respectively. Using this water level data throughout the study period, the energy slope line was calculated by dividing the difference between these two water level elevations over the flow length between two bridges at the exact same time. Figure 2 illustrates the SPB water level recording station.

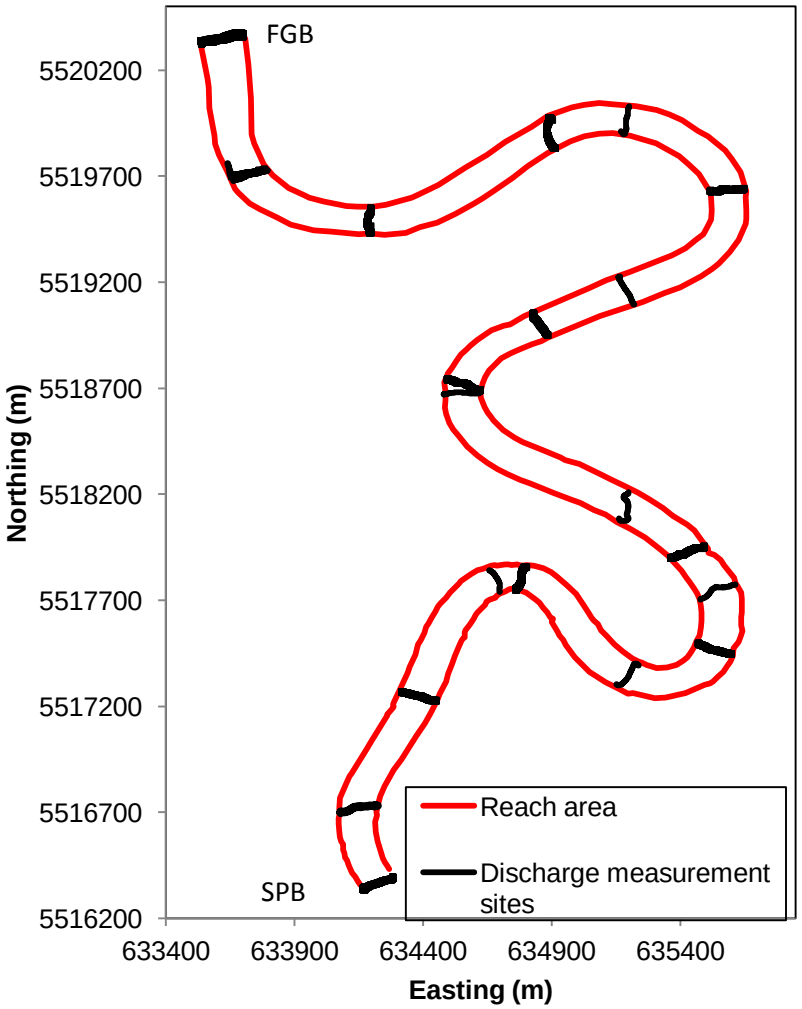


Figure 1. Plan view of ADCP measurements

Figure 2. SPB water level recording station

## 3. DATA PROCCESSING AND DISCUSSION

### 3.1. Water Level Data Processing

Water surface elevation data was collected at the upstream and downstream ends of the study area. The average water surface elevations at each cross section for a single day during the data collection period were used to provide water surface frequency analysis. The elevation range frequency information for SPB during the study period is presented in Table 1. The most frequent water surface elevation of the Red River at this location has a value between 223 and 224 m. Water level frequency information can also describe flow durations which have a major impact on many river processes such as erosion and deposition.

Table 1. Measured water level frequencies at SPB

| Water surface elevation (WSE) (m) | Frequency in percent of time |
|---|---|
| 228-229 | 14 |
| 227-228 | 3 |
| 226-227 | 6 |
| 225-226 | 6 |
| 224-225 | 10 |
| 223-224 | 37 |
| 222-223 | 24 |

Comparing data between water levels at SPB and FGB on the same day and time provides the water surface differences at two boundary ends. The reach was determined to be a part of the river with a small water surface slope. This data was used to develop the water surface profile between two boundary points based on a simple curve fitting method (Equation 1). This equation simply demonstrates the average drop of water surface (WS) in meters, for any typical flow conditions. Since the water surface profile becomes extremely flat in low flow condition, this equation is only valid when the water level at SPB is greater than 222.5 m.

$$[1]\ (\mathrm{FGB})_{\mathrm{WS}} = (\mathrm{SPB})_{\mathrm{WS}} - \{0.0801[(\mathrm{SPB})_{\mathrm{WS}}] - 17.838\}$$

### 3.2. Discharge Data Processing and Stage Curve Development

ADCP discharge measurements were carried out to investigate the effect of seasonal water level on discharge variation and the flow characteristics. Discharge measurements and the flow frequency analysis show that the discharge varied between 50 and 1200 $m^3/s$ over the study period. Table 2 summarizes some key discharges with corresponding water level data at SPB and basic geometric characteristics. In the table, Q is the discharge ($m^3/s$), T is the water surface width (m), A is the area of the cross section ($m^2$), $H_m$ is the maximum flow depth at a given cross section (m), R (=A/P) is the hydraulic radius (m), with P being the wetted perimeter for a given cross section (m), D (=A/T) is the hydraulic depth (m), and T/R is the aspect ratio. Since in all flow conditions the aspect ratio is greater than 20 (T/R > 20), it can be assumed that the Red River is a wide channel.

The discharge and water surface elevation measurements at the SPB cross section were used to develop the stage-discharge rating curve. This rating curve is applicable for a relatively wide flow range. Since the measured data includes bankfull conditions, the rating curve can be used in the flow forecasting model during potential flood events.

Table 2. Key discharges and water levels versus primary geometric properties

| WSE at SPB (m) | Q ($m^3/s$) | Basic geometric characteristic | | | | | |
|---|---|---|---|---|---|---|---|
| | | T (m) | A ($m^2$) | $H_m$ (m) | D (m) | R (m) | T/R |
| 228.74 | 1200 | 159 | 1116 | 10.5 | 6.8 | 7 | 23 |
| 227.9 | 950 | 164 | 997 | 9.5 | 6.1 | 6.8 | 24 |
| 226.7 | 640 | 143 | 759 | 8.1 | 5.3 | 5.7 | 25 |
| 226.5 | 600 | 140 | 734 | 7.9 | 5.2 | 5.5 | 26 |
| 226.1 | 518 | 139 | 684 | 7.5 | 4.9 | 5.3 | 26 |
| 224.9 | 293 | 131 | 528 | 6.3 | 4 | 4.5 | 29 |
| 224.8 | 250 | 131 | 513 | 6.2 | 3.9 | 4.3 | 31 |
| 224.4 | 200 | 123 | 461 | 5.8 | 3.7 | 4.1 | 30 |
| 224.2 | 164 | 127 | 426 | 5.5 | 3.4 | 3.9 | 33 |
| 223.9 | 120 | 128 | 402 | 5.3 | 3.1 | 3.7 | 35 |
| 223.8 | 50 | 115 | 216 | 5.3 | 3.1 | 2.5 | 46 |

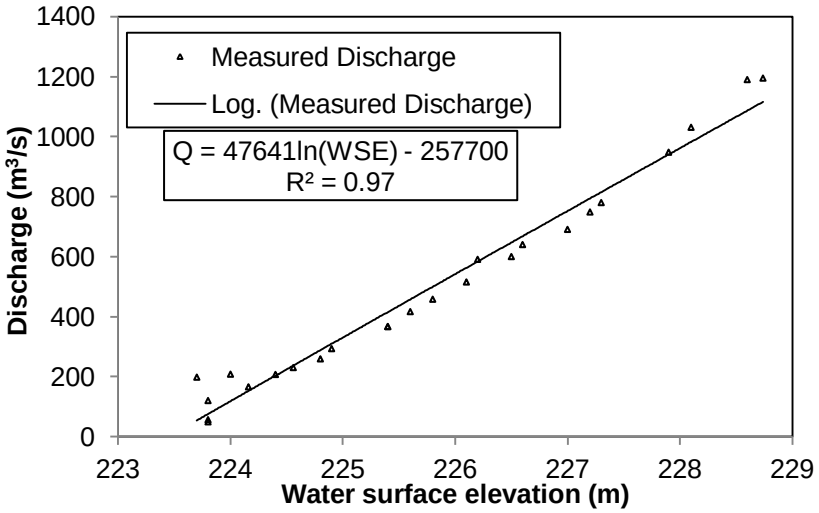


Figure 3. Discharge rating curve for SPB

### 3.3. Average Shear Stress

Reach-averaged shear stress estimation was applied on the basis of momentum principles in one-dimensional uniform, steady flow. This method estimates applied shear stress in the stream-wise direction of a river using Equation 2 (Chow 1959). In this equation, fluid shear stress is proportional to the slope of the channel, the fluid weight in the direction of flow, and the specific weight of fluid.

$$[2]\ \tau_{ave} = \gamma RS$$

Where $\tau_{ave}$ is the mean boundary shear stress (Pa), $\gamma$ is the specific weight of water (N/m$^2$), $S$ is the bed slope which is equal to water surface slope, assuming uniform flow. In this equation the specific weight of water was taken to be $\gamma = 9806$ N/m$^2$.

In order to estimate the average applied shear stress at a given cross section, A, P, and R for each discharge measurement (Q) were computed to obtain water level curve dependent graphs for those parameters based on curve fitting methods. The energy slope line is also required to determine global applied shear stress, and was estimated based on the measured water levels at the reach extremes. Figure 4 presents the calculated mean shear stress at SPB on the basis of water level measurements. Estimated one-dimensional mean boundary shear stresses along the reach ranged from 0.2 to almost 4 Pa. The average shear velocity $(u_*)_{ave}$, which is another primary variable in the hydraulics field can be computed by Equation 3 (Chow 1959).

$$[3]\ (u_*)_{ave} = \sqrt{\frac{\tau_{ave}}{\rho}}$$

Where $\rho$ is the specific mass of water, which is assumed to be 1000 kg/m$^3$. Therefore, the shear velocity ranged from 0.01 to 0.063 m/s (Figure 4). An accurate determination of shear velocity at a river section is fundamental for a various number of river engineering processes such as simulation of velocity distribution, cross sectional shear stress distribution, and total sediment transport load.

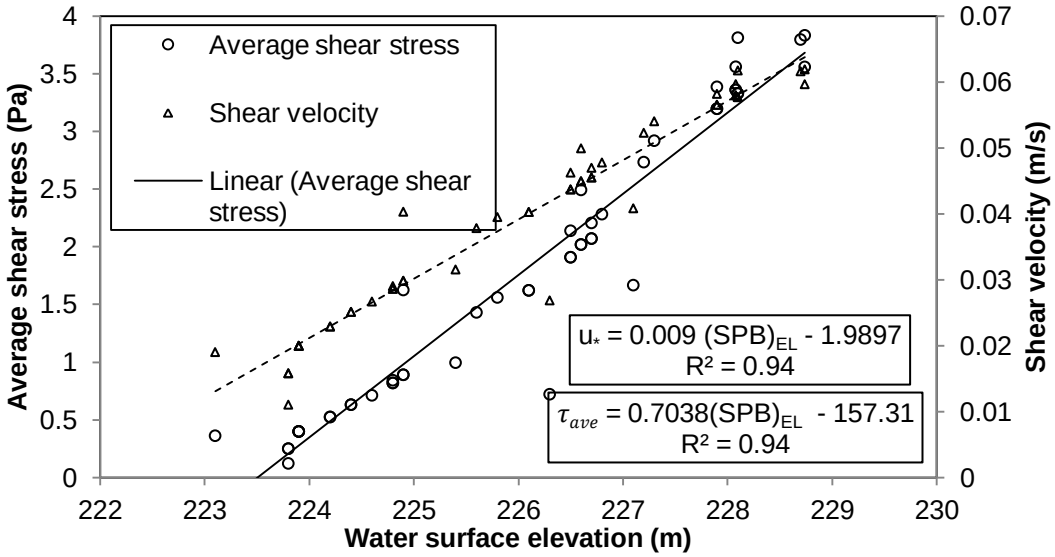


Figure 4. Average shear stress and shear velocity against SPB water level

### 3.4. Velocity Measurement Analysis

Velocity measurement data has the potential to quantify various flow properties. Table 3 summarizes some key discharges and basic hydraulic characteristics using velocity measurement data. In the table, Re ($=\frac{V_{ave}*R}{\vartheta}$) is the Reynolds number, with $\vartheta$ being the kinematic viscosity, Fr ($=\frac{V_{ave}}{\sqrt{g*D}}$) is the Froude number, where g is the gravitational acceleration. Froude and Reynolds numbers are able to classify stream flows, display the energy condition of the river, and provide an overview of the potential for sediment transport and erosion. These dimensionless numbers indicate that all the flow measurements were performed under sub-critical, turbulent flow conditions. The Red River is a deep, turbulent, slow moving river with strong inertial forces and weak gravitational and viscous forces.

The three dimensional measured water velocities at each cross section were used to provide velocity frequency analysis on the basis of water level and discharge. The summary of the velocity frequency information for a range of discharges is presented in Table 4. In this Table, $V_{max}$ and $V_{ave}$ are the measured maximum velocity and the mean velocity (m/s) at a given cross section, respectively.

Table 3. Key discharges versus primary hydraulic properties

| | Basic hydraulic characteristics | | | | |
|---|---|---|---|---|---|
| **Discharge ($m^3/s$)** | **Froude number** | **Reynolds number*$10^6$** | **Specific energy (m)** | **Velocity head (m)** | **Water surface slope*$10^{(-5)}$** |
| 1200 | 0.130 | 7.6 | 7.1 | 0.060 | 5.6 |
| 950 | 0.120 | 6.8 | 6.1 | 0.050 | 4.8 |
| 640 | 0.120 | 4.6 | 5.3 | 0.040 | 3.6 |
| 600 | 0.120 | 4.5 | 5.3 | 0.040 | 3.5 |
| 518 | 0.110 | 4.0 | 5.0 | 0.030 | 3.1 |
| 293 | 0.09 | 2.5 | 4.0 | 0.020 | 2.0 |
| 250 | 0.08 | 2.1 | 3.9 | 0.010 | 1.9 |
| 200 | 0.07 | 1.8 | 3.7 | 0.010 | 1.6 |
| 164 | 0.07 | 1.5 | 3.4 | 0.010 | 1.4 |
| 120 | 0.05 | 1.1 | 3.1 | 0.005 | 1.1 |
| 50 | 0.03 | 0.3 | 1.9 | 0.003 | 1.1 |

Table 4. Summary of frequency-derived velocity statistics versus discharge

| | Average and maximum velocity under different discharge values | | | | | | |
|---|---|---|---|---|---|---|---|
| | **Q = 1200 ($m^3/s$)** | **Q = 950 ($m^3/s$)** | **Q = 750 ($m^3/s$)** | **Q = 600 ($m^3/s$)** | **Q = 518 ($m^3/s$)** | **Q = 294 ($m^3/s$)** | **Q = 231 ($m^3/s$)** |
| $V_{ave}$ | 1.075 | 1.03 | 0.94 | 0.86 | 0.77 | 0.61 | 0.64 |
| $V_{max}$ | 1.36 | 1.32 | 1.2 | 1.1 | 1.00 | 0.8 | 0.8 |
| $\frac{V_{max}}{V_{ave}}$ | 1.26 | 1.28 | 1.27 | 1.28 | 1.29 | 1.31 | 1.28 |

### 3.5. Roughness Coefficients and Roughness Heights

It is obvious that the magnitude and variability of river surface resistance have a great impact on the river discharge capacity, the applied shear stress, sediment transport, and flooding. ADCP measurements were processed to determine global open channel resistance coefficient in terms of Manning's n, as a basis for 2D hydrodynamic modeling calibration. Manning's n is estimated by simplifying the discharge equation for uniform flow (Equation 4) (Chow 1959).

$$[4]\ n = \frac{A * S^{\frac{1}{2}} * R^{\frac{2}{3}}}{Q}$$

In order to perform best professional judgment of the one dimensional reach scale Manning's n value, all the parameters on the right-hand side of equation 4 were computed at all cross sections. The calculation of reach-representative Manning's n for wide ranges of discharge varied from 0.022 to 0.031 ($\mu = 0.025$).

Bed roughness is an important parameter for many applications and numerical model development in fluid mechanics and hydraulics. In open channel flow prediction, a series of equations have been developed in order to examine a link between river roughness height and flow resistance. The most practical equation is on the basis of Manning's value to provide a relationship between roughness coefficient and the surface roughness height (Chen 1991, McGehery and Samuels 2004). This equation is as follows:

$$[5]\ k_s = (25.4 * n)^6$$

The value of the average surface roughness height through the use of Manning's coefficient was 9 cm. Roughness Reynolds number ($k_s^+$) can be calculated using Equation 6

$$[6]\ k_s^+ = \frac{u_* * k_s}{\vartheta}$$

Applying this non-dimensional number for the Red River infers that the Red River is a hydraulically fully rough channel ($k_s^+ > 70$) (Schlichting 1955).

### 3.6. Local Boundary Shear Stress and Hydraulic Shear Stress Distribution

The shear stress distribution at a given cross section is the basic parameter for prediction of sediment transport, erosion and deposition mechanisms, riverbank stability, and other important processes in natural channels. Reynolds number, aspect ratio, and Roughness Reynolds number indicate that the flow regime in the Red River can be considered as a turbulent flow in wide rough open channel. This type of regime can be described by the logarithmic law streamwise vertical distribution. In this study, ADCP data and reach-averaged bed roughness height values were used to estimate the shear stress distribution on the Red River based on the logarithmic law (turbulent flows concept). The ADCP divided the cross section into slices for each flow measurement. Depth-averaged velocity in each vertical slice was obtained by averaging the measured velocities from all cells on the same vertical sample. Local applied shear stresses were calculated by Equation 7 (Schlichting 1955).

$$[7]\ \tau = \frac{\rho * V^2 * f_c}{2}$$

Where $\tau$ = hydraulic shear stress (N/m$^2$), $\rho$ is density of fluid (kg/m3), $V$ is depth-averaged current velocity (m/s), and $f_c$ is current friction factor. Current friction factor can be obtained using Equation 8 (Schlichting 1955).

$$[8]\ f_c = 2\{2.5\left\{\ln\left[\frac{30H}{k_s}\right] - 1\right\}\}^{-2}$$

Where $H$ = water depth (m), and $k_s$ is bed roughness height (m). Figure 5 indicates the hydraulic shear stress distribution at SPB when the discharge was 1200 m$^3$/s. Since the shear distribution on the basis of turbulent flows concept is a function of water depth and water velocity, the distribution using this method is realistic especially close to the piers. In Figure 5 it can be seen that velocity and consequently shear stress close to the piers become smaller even though the depths are significantly deep (red circles).

Average shear stress from cross sectional shear stress distribution was calculated for each measurement. Table 5 shows a comparison between average shear stress calculated by two methods; the turbulent flows concept (Equation 7) and the momentum principle (Equation 2). Relative errors ($\varepsilon$) between these two methods were calculated for each measurement. The average absolute relative error between two methods for this table dataset is 10%, demonstrating that these methods agree closely.

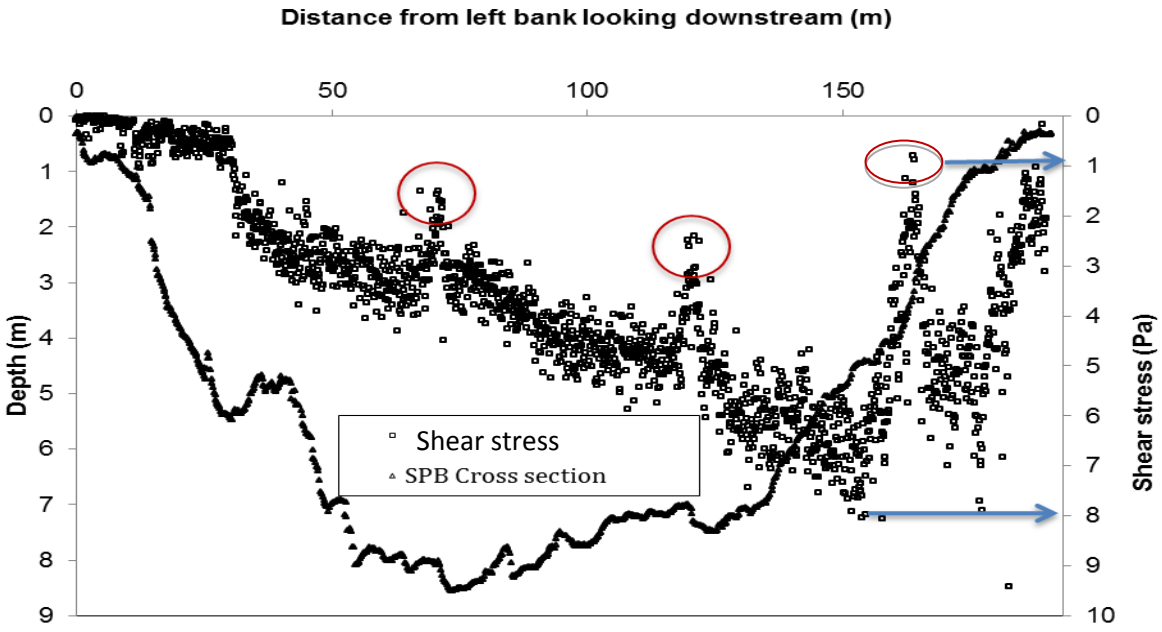


Figure 5. Shear stress distribution at SPB (Q=1200 $m^3/s$)

Table 5. Comparison between two methods for modeling the cross sectional average shear stress

| Average shear stress (Pa) on the basis of | Average shear stress under different discharges | | | |
|---|---|---|---|---|
| | 1208 ($m^3/s$) | 1031 ($m^3/s$) | 948 ($m^3/s$) | 518 ($m^3/s$) |
| Turbulent flows concept | 3.9 | 2.9 | 2.9 | 2.0 |
| Momentum equation | 3.8 | 3.3 | 3.2 | 1.7 |

## 4. CONCLUSION

In this study a combination of ADCP measurements and water surface data collection were used to investigate the characteristics of flow on a reach of the Red River in Winnipeg over a 2 year period. Collected data were analyzed to develop numerical models of river processes including hydrodynamics and sediment transport. In addition, these data were used to develop models that provide suitable results on the basis of the water surface elevation that is simple to measure. The relationship between the water level and discharge, basic geometric parameters, maximum and average velocity, average shear stress, velocity head, and hydraulic grade line were developed. Also, several primary field and calibration variables such as Froude number, Reynolds number, average shear velocity, roughness coefficient, and surface roughness height were determined for a wide range of water levels. These relationships and primary variables provide a better understanding of complicated phenomena such as applied shear stress, erosional and depositional processes, and sediment transport occurring on the Red River.

## 5. ACKNOWLEDGEMENTS

This research was supported by Manitoba Hydro and the Natural Sciences and Engineering Research Council of Canada. The authors would like to thank Mr. Sparrow, Mr. Wall, Mr. Sagan, and Mr. Westervelt for their contributions to the field work for this study.

## 6. REFERENCES

ASCE. 1998. River width adjustment. I: Processes and Mechanisms. *Journal of Hydraulic Engineering,* 124 (9): 881-902.

Chen, C.L. 1991. Unified Theory on Power Laws for Flow Resistance. *Journal of Hydraulic Engineering*, 117(3): 371–389.

Chow, V.T. 1959. *Open-channel hydraulics*, McGraw-Hill, New York, NY, USA.

Ferrick, M. G. & Gatto, L. W. 2005. Quantifying the effect of a freeze–thaw cycle on soil erosion: laboratory experiments. *Earth Surface Processes and Landforms*, Volume 30, pp. 305-326.

Formanek, G., McCool, D. & Papendick, R., 1984. Freeze-thaw and consolidation effects on strength. *Transactions of the ASAE*, 27(6), pp. 1749-1752.

IPCC. 2007. *Climate Change 2007: The Physical Science Basis*, Cambridge University Press, Cambridge, United Kingdom and New York, NY, USA.

Lawler, D.M., Thorn, C.R., and Hooke, J.m. 1997. Chapter 6: Bank erosion and instability. In *Applied Fluvial Geomorphology for River Engineering and Management*, John Wiley and Sons, New York, NY, USA.

McGahey, C., and Samuels, P.G. 2004. River Roughness-the integration of diverse knowledge. *River Flow 2004*, 405-414.

Nam, S., Samuels, P., and Diplas, P. 2004. Effects of spatial variability on the estimation of erosion rates for cohesive riverbanks. *River Flow 2010*, 1309-1314.

RiverSurveyor S5/M9 System Manual Firmware Version 1.50., 2011. SonTek, a Division of YSI Inc. San Diego, CA, USA.

Schlichting, H. 1955. Boundary- layer Theory, McGraw-Hill, New York, NY, USA.

Simon, A., Curini, A., Darby, S.E., and Langendoen, E. J. 2000. Bank and near-bank processes in an incised channel. *Geomorphology* 33(3-4): 193-217.

Trimble, S.W.1997. Contribution of stream channel erosion to sediment yield from an urbanizing watershed. *Science* 278(5342): 1442-1444.